



ELSEVIER

Seminars in  
**NUCLEAR  
MEDICINE**

# Therapeutic Radionuclides: Biophysical and Radiobiologic Principles

Amin I. Kassis, PhD

Although the general radiobiologic principles underlying external beam therapy and radionuclide therapy are the same, there are significant differences in the biophysical and radiobiologic effects between the 2 types of radiation. In addition to the emission of particulate radiation, targeted radionuclide therapy is characterized by (1) extended exposures and, usually, declining dose rates; (2) nonuniformities in the distribution of radioactivity and, thus, absorbed dose; and (3) particles of varying ionization density and, hence, quality. This review explores the special features that distinguish the biologic effects consequent to the traversal of charged particles through mammalian cells. It also highlights what has been learned when these radionuclides and radiotargeting pharmaceuticals are used to treat cancers.

Semin Nucl Med 38:358-366 © 2008 Elsevier Inc. All rights reserved.

For almost a hundred years, the scientific and medical communities have used radionuclides for therapy. The hopes for employing unsealed sources, however, are still mainly unrealized. The problem has 3 components. The first is the availability of radionuclides with appropriate physical properties. The second involves the interaction between the radionuclide and its biologic environment, ie, the radiation biology of the decaying moiety. The third is the identification of carrier molecules with which to target such radionuclides to tumors. In the case of the radionuclide, one must consider its mode of decay, including the nature of the particulate radiations and their energies, its physical half-life, and its chemistry in relation to the carrier molecule. In the case of the carrier, one must define its stability and specificity; the biologic mechanisms that will bind it to the targeted cells, including the number of accessible sites and the affinity of the carrier to these sites, the stability of the receptor-carrier-molecule complex, the distribution of sites among cells (both target and nontarget), the relationship of site appearance to the cell cycle, and the microenvironment of the target (for a tumor, its vascularity, vascular permeability, oxygenation, microscopic organization and architecture, including the mobility of the cells, their location and accessibility to intralymphatic, intraperitoneal, intracerebral and intramedullary

routes). In addition, the outcome is dependent on certain biologic responses that are outlined herein.

In this review, both the special features that characterize the biologic effects consequent to the traversal of charged particles through mammalian cells and the state of knowledge concerning the use of these radionuclides to treat cancers will be emphasized. The current status of radionuclide-based therapies will also be reviewed.

## Particulate Radiation

### Energetic Particles

In general, the distribution of therapeutic radiopharmaceuticals within a targeted solid tumor is not homogeneous. This is mainly a result of (1) the inability of the radiolabeled molecules to penetrate uniformly dissimilar regions within a solid tumor mass; (2) the high interstitial pressure of solid tumors; and/or (3) differences in the binding-site densities of tumor cells. In the case of radiopharmaceuticals labeled with energetic alpha-particle and beta-particle emitters (range of emitted particle  $\gg$  than diameter of the targeted cell), such nonuniformity will lead to dosimetric nonhomogeneities, ie, major differences in the absorbed doses to individual tumor cells. Consequently, the mean absorbed dose is less likely to be a good predictor of radiotherapeutic efficacy.

### Alpha-Particle Emitters

During the past 40 years, the therapeutic potential of several alpha-particle-emitting radionuclides has been assessed. These particles (1) are positively charged with a mass and charge equal to that of the helium nucleus, their emission

Department of Radiology, Harvard Medical School, Boston, MA.

Supported by NIH 5 R01 CA015523.

Address reprint requests to Amin I. Kassis, PhD, Department of Radiology, Harvard Medical School, Armenise Building, 200 Longwood Avenue, Boston, MA 02115. E-mail: [amin\\_kassis@hms.harvard.edu](mailto:amin_kassis@hms.harvard.edu)



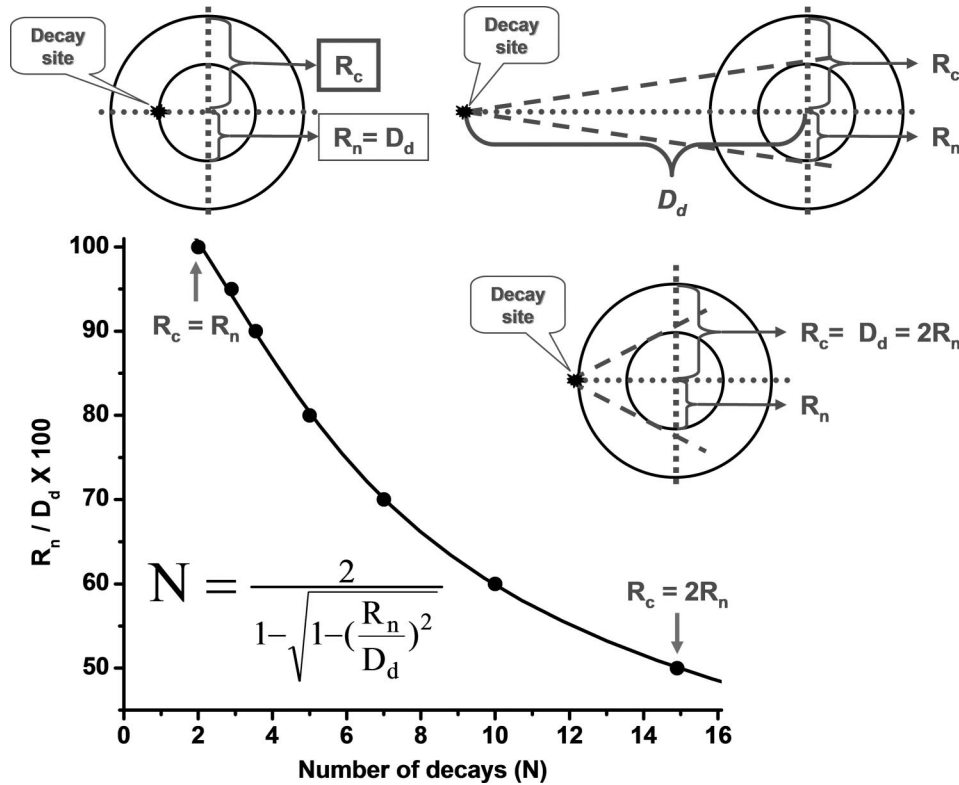


**Figure 3** Number of radioactive atoms required to ensure traversal of cell nucleus by one energetic particle as function of distance from center of cell. Nuclear radius to distance of decaying atom (percentage) is plotted as function of number of decays ( $N$ ).  $R_c$ : cell radius;  $R_n$ : nuclear radius;  $D_d$ : distance of decaying atom from center of cell for one nuclear traversal. Note that (1) nuclear localization of radioactive atom is the only condition that will lead to one traversal per decaying atom; (2) when decaying atoms are on nuclear membrane,  $\geq 2$  radioactive atoms are needed for one nuclear traversal; and (3) when decaying atoms are localized on cell membrane and diameter of cell is twice that of nucleus,  $>15$  radioactive atoms are necessary to ensure one nuclear traversal.

age of 5 to 30 Auger electrons, with energies ranging from a few eV to approximately 1 keV, are emitted per decaying atom.<sup>3</sup> In addition to producing low-energy electrons, this form of decay leaves the daughter atom with a high positive charge resulting in subsequent charge-transfer processes.

The very low energies of Auger electrons have 2 major consequences: (1) these light, negatively ( $-1$ ) charged particles travel in contorted paths and their range in water is from a fraction of a nanometer up to  $\sim 0.5 \mu\text{m}$  (Table 1); and (2) multiple ionizations (LET: 4-26 keV/ $\mu\text{m}$ ) occur in the immediate vicinity (few nanometers) of the decay site (Fig. 4),<sup>4</sup> reminiscent of those observed along the path of an alpha particle.<sup>3</sup> Finally, the short range of Auger electrons necessitates their close proximity to the radiosensitive target (DNA) for radiotherapeutic effectiveness (Table 1). This is essentially a consequence of the precipitous drop in energy density as a function of distance in nanometers.<sup>5-7</sup>

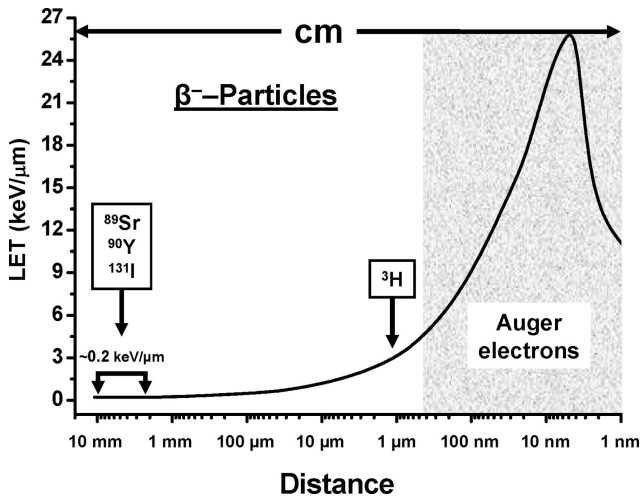


**Figure 4** LET along paths of energetic beta particles and Auger electrons as function of traversed distance.

### Radiobiology

The deposition of energy by ionizing radiation in mammalian cells is a random process. The absorption of energy in such cells can induce certain molecular modifications that may lead to cell death. Although this process is stochastic in nature, the death of a few cells within a tissue or an organ will not have, in general, a significant effect on function. However, as the dose increases, more cells will die with the eventual impairment of tissue/organ function.<sup>8</sup>

## Molecular Lesions

DNA is the principal target responsible for radiation-induced biologic effects. A number of different lesions occur (eg, single-strand breaks [SSB], double-strand breaks [DSB], base damage, DNA–protein cross-links, multiply damaged sites [MDS]). These changes may be produced by the direct ionization of DNA (direct effect) or by the interaction of free radicals with DNA (indirect effect, mostly hydroxyl radicals produced in water molecules that diffuse several nanometers). Most of these lesions are repaired with high fidelity, the exceptions being DSB and MDS.

The distribution of ionizations within DNA and the type of damage created depend on the nature of the incident particle and its energy. Alpha particles produce a high density along a linear path (Fig. 5, bottom); energetic beta particles, infrequent ionizations along a linear path (Fig. 5, top); low-energy electrons, frequent ionizations along an irregular path; and Auger cascades, clusters of high ionization density (Fig. 5, center). Double-strand breaks generated by high specific ionization (eg, alpha particles and Auger-electron cascades) are less repairable than SSBs (eg, created by more sparsely ionizing radiation).

## Cellular Responses

### Clonal Survival

When mammalian cells are acutely exposed (high dose rate) to ionizing radiation, their ability to divide indefinitely declines as a function of radiation dose. The shape of the survival curve (Fig. 6) depends on the density of ionizations. For

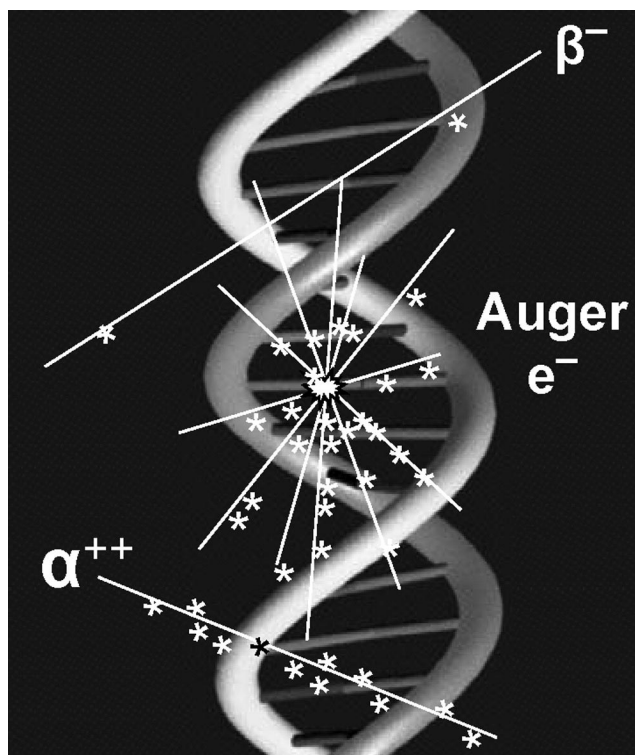


**Figure 5** Schematic representation of ionization densities produced along tracks of energetic beta particles, Auger electrons, and alpha particles.

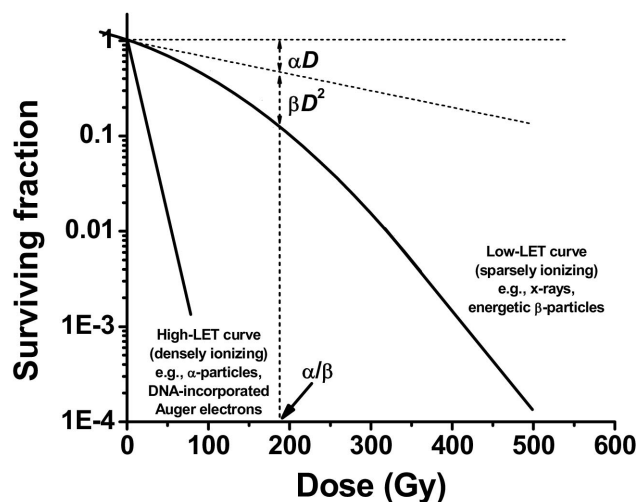


**Figure 6** Mammalian cell survival curves after high- and low-LET irradiation. With high-LET radiation (alpha and nonenergetic electrons), curve shows exponential decrease in survival; with low-LET radiation (energetic electrons), curve exhibits a shoulder.

densely ionizing radiation (alpha particles and Auger-electron cascades), the logarithmic response is linear ( $-\ln SF = \alpha D$ ), where  $SF$  is the survival fraction,  $\alpha$  is the slope, and  $D$  is the absorbed dose. For sparse radiation, the logarithmic response is linear-quadratic ( $-\ln SF = \alpha D + \beta D^2$ ), where  $\alpha$  is the rate of cell kill by a single-hit mechanism,  $D$  is the dose delivered, and  $\beta$  equals the rate of cell kill by a double-hit mechanism (the  $\beta D^2$  term is thought to represent accumulated and repairable damage). This type of survival curve is routinely observed when mammalian cells are exposed to low-LET radiation (eg, photons, energetic beta particles, extranuclear Auger electrons). When the dose rate is low, as often occurs with radionuclides, the  $\alpha$  term predominates. It is important to note that the  $\alpha$ -to- $\beta$  ratio represents the dose at which cell killing by the linear and quadratic components is equal, ie, when  $\alpha D = \beta D^2$  ( $D = \alpha/\beta$ ).

Because sparsely ionizing radiation produces repairable sublethal damage, both the shape of the dose–response curve and the acuteness of the slope are sensitive to dose rate. Consequently, lower dose rates are less damaging than higher ones. In radionuclide therapy this is particularly important when the physical half-life of the isotope is somewhat long. Thus, as with fractionated external beam therapy, the total dose from continuous low-dose radionuclide therapy is less effective than a single dose of the same magnitude, ie, for a comparable biologic effect, a larger dose is required.<sup>9</sup>

Whereas it is clear that radionuclides whose decay results in a purely exponential decrease in cell survival (every decay leads to a corresponding decrease in survival) are preferable for radiotherapy, the exponential nature of linear and linear-quadratic survival curves has important implications. In essence, it indicates that only very high doses will reduce the number of viable cancer cells in a macroscopic tumor to less than one. Therefore, no dose will be sufficiently large to eradicate 100% of the clonogenic cells with certainty, espe-

cially since it will always be limited by normal tissue tolerance.

### Division Delay and Programmed Cell Death

Irradiation of dividing mammalian cells leads to a delay in their progression through their cell cycle. However, this delay is reversible and its length is dose-dependent. Furthermore, it occurs only at specific points in the cell cycle and is similar for both surviving and nonsurviving cells: maximum delay is observed when premitotic  $G_2$  cells are irradiated, little delay is observed in  $G_1$  cells, moderate delay in S cells, and cells in mitosis continue through division basically undisturbed. Consequently, the irradiation of such dividing mammalian cells leads to their accumulation at the  $G_2/M$  boundary and a change in their mitotic index.

Division delay allows irradiated cells time to determine their fate. When cells are irradiated and DNA is damaged, the damage is sensed and various genes are activated. Cells held at checkpoints await repair of DNA, and then proceed through the cell cycle. Alternatively, damage may be non-reparable, and the cells are induced to undergo programmed cell death or apoptosis. However, because not all cells are born equal, the apoptotic response is varied. For example, lymphoid tumor cells are more likely to undergo apoptosis than epithelial cells. This may account for the success of radioimmunotherapy in certain lymphomas, whereas, in epithelial cells, apoptosis appears to account for only a small portion of clonal cell death.

### Oxygen Enhancement Ratios

It is well known that oxygen radiosensitizes mammalian cells to the damaging effects of radiation. Hypoxic cells can be up to 3-fold more radioresistant than well-oxygenated cells, because oxygen enhances free radical formation and/or it may block reversible and repairable chemical alterations. The oxygen effect is maximal for low-ionization-density radiation (photons and high-energy beta particles) and minimal for high-LET radiation (alpha particles, low-energy electrons including Auger-electron cascades). In the former instance, the presence of hypoxic regions within tumors is believed to be a major cause of radiotherapeutic failure.

### Bystander Effect

Radiation-induced bystander effects refer to biologic responses occurring in cells that are not traversed by an ionizing radiation track and, thus, are not subject to energy deposition events, ie, the response(s) take place in unirradiated cells. As such, these bystander effects are somehow communicated from an irradiated cell to an unirradiated cell, via cell-to-cell gap junction communication<sup>10</sup> and/or by the secretion or shedding of soluble factors whose precise nature is unknown, although reactive oxygen and nitrogen species and various cytokines have been implicated.<sup>11-15</sup>

Originally observed with external alpha-particle beams in vitro, the phenomenon has also been observed in subcutaneous tumors.<sup>14,16,17</sup> These observations have negated a central tenet of radiobiology that damage to cells is caused only by direct ionizations and/or by free radicals generated as a consequence of the deposition of energy within the nuclei of

mammalian cells. The importance of the bystander effect as an enhancer of radiotherapeutic efficacy is yet to be determined.

### Self-Dose, Cross-Fire, and Nonuniform Dose Distribution

When radionuclides are used for therapy, cells may be irradiated by decays taking place on or within the targeted cells (self-dose) or in neighboring or distant cells (cross-fire). Because of geometric factors (Fig. 3), the self-dose from energetic alpha and beta particles depends on their position on or within the tumor cell, whereas that from Auger-electron emitters depends mainly on the proximity of the decaying atom to DNA.

In targeted radionuclide therapy, the distribution of radioactivity and, hence, the absorbed dose tend to be nonuniform. Consequently, higher doses are required to sterilize targeted cells. Humm<sup>18,19</sup> has calculated that the difference in dose needed for a similar decrease in survival fraction with uniform and nonuniform dose distributions of alpha-particle-emitting radionuclides is greater ( $\Delta\alpha > \Delta\beta$ ) than that for energetic beta particles (Fig. 7). O'Donoghue<sup>20</sup> also has described a mathematical model that examines the impact of dose nonuniformity and dose-rate effects on therapeutic response. This model predicts that (1) a nonuniform dose distribution grows proportionately less effective as the absorbed dose increases; (2) the surviving fraction increases for any mean absorbed dose as the absorbed dose distribution becomes less uniform; and (3) the difference in survival fraction—consequent to a uniform versus nonuniform dose—is more pronounced as the radiosensitivity of tumor cells increases.

### Half-Life

Because many biologic responses to radiation are sensitive to dose rate as well as total dose, the physical half-life ( $T_{1/2P}$ ) of the radionuclide employed and the biological half-life ( $T_{1/2B}$ )

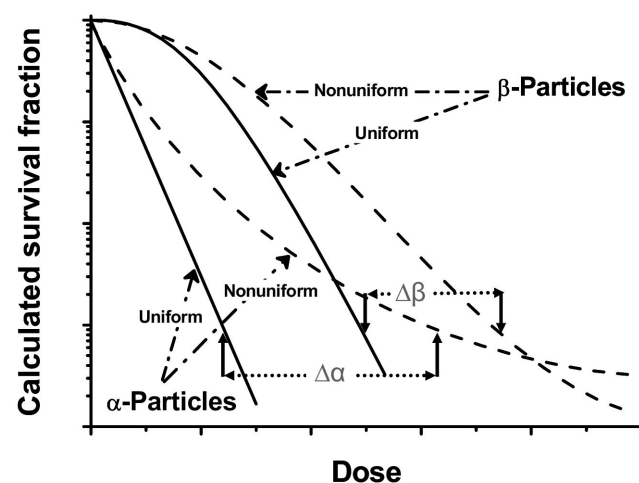


**Figure 7** Schematic representation of relationship between mammalian cell survival and alpha- and beta-particle-emitter distribution as a function of dose. Solid lines, uniform irradiation; broken lines, nonuniform irradiation.

in tumor and normal tissue affect the response of the tumor. For a radiopharmaceutical with an infinite residence time in a tumor, a radionuclide with a long physical half-life will deliver more decays than one with a short half-life if both have the same initial radioactivity. There is also a striking difference in the time-dependent dose rate delivered by the 2. For example, if the number of radionuclide atoms per unit of tumor mass is  $n$  and the energy emitted (and absorbed) per decay is  $E$ , then the absorbed-dose rate is proportional to  $nE/T$  where  $T$  is the half-life. The ratio  $E/T$  is an important indicator of the intrinsic radiotherapeutic potency of the radionuclide.<sup>21</sup> From a radiobiologic standpoint, higher dose rates delivered over shorter treatment times are more effective than lower dose rates delivered over longer periods. Thus, a radionuclide with a shorter half-life will tend to be more biologically effective than one with a similar emission energy but longer half-life.

## Experimental Therapeutics

### Energetic Particle Emitters

#### Alpha-Particle Emitters

The application of alpha-particle-emitting radionuclides as targeted therapeutic agents continues to be of interest. When such radionuclides are selectively accumulated in the targeted tissues (eg, tumors), their decay should result in highly localized energy deposition in the tumor cells and minimal irradiation of surrounding normal host tissues.<sup>22,23</sup>

The investigation of the therapeutic potential of alpha-particle emitters has focused mainly on astatine-211 (<sup>211</sup>At), bismuth-212 (<sup>212</sup>Bi), bismuth-213 (<sup>213</sup>Bi), radium-223 (<sup>223</sup>Ra), and actinium-225 (<sup>225</sup>Ac) (Table 2).<sup>22</sup> In vitro studies<sup>24,25</sup> have shown that the decrease in mammalian cell survival after exposure to uniformly distributed alpha particles from such radionuclides is monoexponential but that, as predicted theoretically<sup>19</sup> and shown experimentally,<sup>1</sup> these curves develop a tail when the dose is nonuniform (Fig. 7). Such studies have also indicated that the traversal of 1 to 4 of these high-LET alpha particles through a mammalian cell nucleus will kill the cell.<sup>1,24,25</sup> In comparison, because the LET of negatrons emitted by the decay of energetic beta emitters used for tumor therapy is  $\sim 0.2$  keV/ $\mu\text{m}$  (Fig. 4), thousands of beta particles must traverse a cell nucleus for its sterilization.<sup>26</sup>

**Table 2 Alpha-Particle Emitters: Physical Properties**

Radionuclide	$E_{av}$ (MeV)*	$R_{av}$ ( $\mu\text{m}$ )†	Half-Life
<sup>211</sup> At	6.79	60	7.2 hours
<sup>213</sup> Bi	8.32	84	46 min
<sup>223</sup> Ra	5.64	45	11.43 days
<sup>225</sup> Ac	6.83	61	10 days

\*Mean energy of alpha particles emitted per disintegration.<sup>22</sup>

†Mean range of alpha particles calculated using second order polynomial regression fit (data from the International Commission on Radiation Units and Measurements<sup>23</sup>):

$R = 3.87E + 0.75E^2 - 0.45$ , where  $R$  is the range ( $\mu\text{m}$ ) in unit density matter and  $E$  is the alpha-particle energy (MeV).

**Table 3 Beta-Particle Emitters: Physical Properties**

Radionuclide	Half-Life	$E\beta^-_{(max)}$ (keV)*	$R\beta^-_{(max)}$ (mm)†
<sup>33</sup> P	25.4 days	249	0.63
<sup>177</sup> Lu	6.7 days	497	1.8
<sup>67</sup> Cu	61.9 hours	575	2.1
<sup>131</sup> I	8.0 days	606	2.3
<sup>186</sup> Re	3.8 days	1077	4.8
<sup>165</sup> Dy	2.3 hours	1285	5.9
<sup>89</sup> Sr	50.5 days	1491	7.0
<sup>32</sup> P	14.3 days	1710	8.2
<sup>166</sup> Ho	28.8 hours	1854	9.0
<sup>188</sup> Re	17.0 hours	2120	10.4
<sup>90</sup> Y	64.1 hours	2284	11.3

\*Maximum energy of beta particles emitted/disintegration.

†Range ( $\mu\text{m}$ ) for electrons with  $E = 0.02$ -100 keV calculated using Cole's equation<sup>4</sup>:

$R = 0.043(E + 0.367)^{1.77} - 0.007$ , where range (mm) for electrons with  $E$  (MeV) calculated using second order fits (data from the International Commission on Radiation Units and Measurements<sup>23</sup>):

$R_{(0.1-0.5 \text{ MeV})} = 2.4E + 2.86E^2 - 0.14$

$R_{(0.5-2.5 \text{ MeV})} = 5.3E + 0.0034E^2 - 0.93$ .

The therapeutic potential of alpha-particle emitters in tumor-bearing animals has also been assessed.<sup>27-31</sup> For example, Bloomer and coworkers<sup>27</sup> have reported a dose-related prolongation in median survival when mice bearing an intraperitoneal murine ovarian tumor are treated with <sup>211</sup>At-tellurium colloid administered directly into the peritoneal cavity. Whereas this alpha-particle-emitting radiocolloid is curative without serious morbidity, beta-particle-emitting radiocolloids (phosphorus-32, dysprosium-165, yttrium-90) are much less efficacious. In another set of in vivo studies examining the therapeutic efficacy of <sup>225</sup>Ac-labeled internalizing antibodies, McDevitt and coworkers<sup>32</sup> have demonstrated the therapeutic efficacy of <sup>213</sup>Bi-labeled internalizing antibodies in mice bearing solid prostate carcinoma or disseminated lymphoma.

#### Beta-Particle Emitters

Historically, studies of radionuclide-based tumor therapy have been performed mainly with energetic beta-particle emitters. The exposure of cells in vitro to beta particles leads, in general, to survival curves that have a distinct shoulder and a  $D_0$  of several thousand decays.<sup>26,33</sup> Despite the rather low in vitro cytotoxicity, these radionuclides continue to be pursued for targeted therapy, mainly due to their availability and favorable physical characteristics (eg, energy and range of the emitted electrons leading to cross-fire irradiation; physical half-lives compatible with biologic half-lives of the carrier molecules; Table 3).<sup>23</sup> As mentioned above, the main advantage of cross-fire is that it negates the necessity of the radiotherapeutic agent's being present within each of the targeted cells, ie, it counteracts a certain degree of heterogeneity. Since the ionization densities of energetic electrons are low, however, the delivery of an effective therapeutic dose to the targeted tissue necessitates that (1) the distances between these foci are equal to or less than twice the maximum range of the

emitted energetic beta particles; and (2) the concentration of the radiotherapeutic agent within each focus is sufficiently high to produce a cumulative cross-fire dose of  $\sim 10,000$  cGy to all the targeted cells. Because dose is inversely proportional to the square of distance, the concentration of the therapeutic agent needed to deposit such cytotoxic doses increases many fold with an increase in nonuniform, radionuclide distribution.

Experimentally, investigators have assessed the therapeutic efficacy of  $^{131}\text{I}$ -labeled monoclonal antibodies in small tumor-bearing rodents. These studies have shown that when such radiopharmaceuticals localize in high concentrations within solid tumors, they are therapeutically quite efficacious.<sup>34</sup> Thus, even when iodine-131 is not-so-uniformly distributed within a tumor, the decay of this radionuclide can lead to sterilization of small tumors in mice so long as it is present in sufficiently high concentrations. Similar results have been reported with radiopharmaceuticals labeled with other beta-particle-emitting isotopes, in particular yttrium-90<sup>35-37</sup> and copper-67.<sup>38</sup> An important outcome of these findings has been the introduction of  $^{131}\text{I}$ - and  $^{90}\text{Y}$ -labeled antibodies in the clinic.

### Low-Energy Electron Emitters

The therapeutic potential of radionuclides that decay by EC and/or IC has been established, for the most part, with iodine-125. Studies with this and other Auger-electron-emitting radionuclides (Table 4) have shown that (1) multiple electrons are emitted per decaying atom; (2) the distances traversed by these electrons are mainly in the nanometer range; (3) the LET of the electrons is  $>20$ -fold higher than that observed along the tracks of energetic ( $>50$  keV) beta particles (Fig. 4); and (iv) many of the emitted electrons dissipate their energy in the immediate vicinity of the decaying atom and deposit  $10^6$  to  $10^9$  rad/decay within a few-nanometer sphere around the decay site.<sup>3</sup> From a radiobiologic prospective, the tridimensional organization of chromatin within the mammalian cell nucleus involves many structural level compactions (eg, nucleosome, 30-nm chromatin fiber, chromonema fiber) whose dimensions are within the range of these high-LET (4-26 keV/ $\mu\text{m}$ ), low-energy ( $\leq 1.6$  keV), short-range ( $\leq 150$  nm) electrons. Therefore, the toxicity of Auger-emitting radionuclides is expected to depend critically

on close proximity of the decaying atom to DNA and to be quite high. These predictions are substantiated by in vitro studies showing that (1) the decay of Auger-electron emitters covalently bound to nuclear DNA leads to monoexponential decreases in survival<sup>6,39</sup>; (2) the curves may or may not exhibit a shoulder when the decaying atoms are not covalently bound to nuclear DNA<sup>40-42</sup>; and (3) in general, intranuclear decay accumulation is highly toxic ( $D_0 = \sim 100$ -500 decays/cell), whereas decay within the cytoplasm or extracellularly produces no extraordinary lethal effects, and these survival curves resemble those observed with x-rays (have a distinct shoulder).<sup>3</sup>

The radiotoxicity of the Auger-electron emitter iodine-125 has been compared with that of the energetic beta-particle emitter iodine-131<sup>26</sup> in mammalian cells in vitro. Unlike the low-LET type of survival curve (with shoulder) obtained following the decay of beta-emitting iodine-131 in DNA, a high-LET curve (with no shoulder) is observed with iodine-125. Additionally, the slope of the latter curve is much steeper than that of the former. In contrast, the decay of iodine-125 in the cytoplasm is much less ( $\sim 80$ -fold) efficient at cell killing.<sup>41</sup> Constantini and coworkers<sup>43</sup> have modified a monoclonal antibody with a nuclear localization peptide sequence, labeled it with indium-111, and have shown a 6-fold enhancement in the radiotoxicity of the antibody to breast cancer cells. Reske and coworkers<sup>44</sup> have demonstrated that the inhibition of thymidylate synthetase, following pretreatment with the antimetabolite fluorodeoxyuridine, leads to a 20-fold increase in radiotoxicity of the  $^{125}\text{I}$ -labeled thymidine analog iodothiodeoxythymidine. Earlier in vitro and in vivo (tumor-bearing rats and cancer patients) studies had similarly shown enhanced uptake and toxicity of  $^{123}\text{I}$ UdR and  $^{125}\text{I}$ UdR by tumors cells.<sup>45,46</sup> Such results support the notion that the biologic effects of an Auger-electron emitter are strongly dependent on its intracellular localization, in particular its proximity to DNA.

The extreme degree of cytotoxicity observed with DNA-incorporated Auger-electron emitters has been exploited in experimental radionuclide therapy. In most of these in vivo studies, the thymidine analog 5-iodo-2'-deoxyuridine (IUdR) has been used.<sup>45,47,48</sup> and the effects have shown excellent therapeutic efficacy. For example, the injection of

**Table 4 Auger-Electron Emitters: Physical Properties**

Radionuclide (#)*	Half-Life	Total Electron Yield Per Decay		
		"Long"-Range Electrons (%)	"Short"-Range Electrons (%)	"Very Short"-Range Electrons (%)
$^{125}\text{I}$ (20)	60.5 days	20 (98)	18 (86)	8 (39)
$^{123}\text{I}$ (11)	13.3 hours	11 (98)	10 (89)	5 (40)
$^{77}\text{Br}$ (7)	57 hours	7 (100)	6 (95)	3 (51)
$^{111}\text{In}$ (15)	3 days	15 (98)	14 (91)	8 (53)
$^{195\text{m}}\text{Pt}$ (36)	4 days	33 (92)	33 (79)	7 (19)
	Range:	$<0.5 \mu\text{m}$	$<100 \text{ nm}$	$<2 \text{ nm}$
	LET†:	4 to 26 keV/ $\mu\text{m}$	9 to 26 keV/ $\mu\text{m}$	$<18 \text{ keV}/\mu\text{m}$

\*Average number of electrons emitted/decay.

†Fit of data by Cole.<sup>4</sup>

$^{125}\text{I}$ UdR into mice bearing an intraperitoneal ascites ovarian cancer has led to a 5-log reduction in tumor cell survival.<sup>47</sup> Similar effects occur with  $^{123}\text{I}$ UdR.<sup>48</sup> Therapeutic doses of  $^{125}\text{I}$ UdR injected intrathecally into rats with intrathecal tumors significantly delay the onset of paralysis, as exemplified by a 5- to 6-log tumor cell kill and the curing of ~30% of the tumor-bearing rats.<sup>45</sup>

## Conclusions

The increase in our understanding of the dosimetry and the therapeutic potential of various modes of radioactive decay has heightened the possibility of using radiolabeled carriers in cancer therapy. Moreover, as a consequence of the great strides in genomics, the development of more precise targeting molecules is at hand. Further progress in the field of targeted radionuclide therapy is being made by the judicious design of radiolabeled molecules that match the physical and chemical characteristics of both the radionuclide and the carrier molecule with the clinical character of the tumor.

## References

- Walicka MA, Vaidyanathan G, Zalutsky MR, et al: Survival and DNA damage in Chinese hamster V79 cells exposed to alpha particles emitted by DNA-incorporated astatine-211. *Radiat Res* 150:263-268, 1998
- Goddu SM, Howell RW, Rao DV: Cellular dosimetry: absorbed fractions for monoenergetic electron and alpha particle sources and S-values for radionuclides uniformly distributed in different cell compartments. *J Nucl Med* 35:303-316, 1994
- Kassis AI: The amazing world of Auger electrons. *Int J Radiat Biol* 80:789-803, 2004
- Cole A: Absorption of 20-eV to 50,000-eV electron beams in air and plastic. *Radiat Res* 38:7-33, 1969
- Kassis AI, Adelstein SJ, Haydock C, et al: Radiotoxicity of  $^{75}\text{Se}$  and  $^{35}\text{S}$ : theory and application to a cellular model. *Radiat Res* 84:407-425, 1980
- Kassis AI, Adelstein SJ, Haydock C, et al: Lethality of Auger electrons from the decay of bromine-77 in the DNA of mammalian cells. *Radiat Res* 90:362-373, 1982
- Kassis AI, Sastry KSR, Adelstein SJ: Intracellular localisation of Auger electron emitters: Biophysical dosimetry. *Radiat Prot Dosimetry* 13: 233-236, 1985
- Kassis AI, Adelstein SJ: Does nonuniformity of dose have implications for radiation protection? *J Nucl Med* 33:384-387, 1992
- Barendsen GW: LET dependence of linear and quadratic terms in dose-response relationships for cellular damage: Correlations with the dimensions and structures of biological targets. *Radiat Prot Dosimetry* 31:235-239, 1990
- Azzam EI, de Toledo SM, Little JB: Direct evidence for the participation of gap junction-mediated intercellular communication in the transmission of damage signals from  $\alpha$ -particle irradiated to nonirradiated cells. *Proc Natl Acad Sci USA* 98:473-478, 2001
- Narayanan PK, Goodwin EH, Lehnert BE:  $\alpha$  particles initiate biological production of superoxide anions and hydrogen peroxide in human cells. *Cancer Res* 57:3963-3971, 1997
- Narayanan PK, LaRue KEA, Goodwin EH, et al: Alpha particles induce the production of interleukin-8 by human cells. *Radiat Res* 152:57-63, 1999
- Iyer R, Lehnert BE: Factors underlying the cell growth-related bystander responses to  $\alpha$  particles. *Cancer Res* 60:1290-1298, 2000
- Kishikawa H, Wang K, Adelstein SJ, et al: Inhibitory and stimulatory bystander effects are differentially induced by iodine-125 and iodine-123. *Radiat Res* 165:688-694, 2006
- Sgouros G, Knox SJ, Joiner MC, et al: MIRD continuing education: Bystander and low-dose-rate effects: Are these relevant to radionuclide therapy? *J Nucl Med* 48:1683-1691, 2007
- Xue LY, Butler NJ, Makrigiorgos GM, et al: Bystander effect produced by radiolabeled tumor cells *in vivo*. *Proc Natl Acad Sci USA* 99:13765-13770, 2002
- Boyd M, Ross SC, Dorrens J, et al: Radiation-induced biologic bystander effect elicited *in vitro* by targeted radiopharmaceuticals labeled with  $\alpha$ -,  $\beta$ -, and Auger electron-emitting radionuclides. *J Nucl Med* 47:1007-1015, 2006
- Humm JL, Cobb LM: Nonuniformity of tumor dose in radioimmunotherapy. *J Nucl Med* 31:75-83, 1990
- Humm JL, Chin LM, Cobb L, et al: Microdosimetry in radioimmunotherapy. *Radiat Prot Dosimetry* 31:433-436, 1990
- International Commission on Radiation Units and Measurements: Absorbed-Dose Specification in Nuclear Medicine, Report 67. *J ICRU* 2:1-110, 2002
- O'Donoghue JA: The impact of tumor cell proliferation in radioimmunotherapy. *Cancer* 73:974-980, 1994
- Kocher DC: Radioactive Decay Data Tables: A Handbook of Decay Data for Application to Radiation Dosimetry and Radiological Assessments. Vol DOE/TIC-11026. Springfield, VA, National Technical Information Center, US Department of Energy, 1981
- International Commission on Radiation Units and Measurements: Stopping Powers and Ranges for Protons and Alpha Particles, Report 49. Bethesda, MD, International Commission on Radiation Units and Measurements, 1993
- Kassis AI, Harris CR, Adelstein SJ, et al: The *in vitro* radiobiology of astatine-211 decay. *Radiat Res* 105:27-36, 1986
- Charlton DE, Kassis AI, Adelstein SJ: A comparison of experimental and calculated survival curves for V79 cells grown as monolayers or in suspension exposed to alpha irradiation from  $^{213}\text{Bi}$  distributed in the growth medium. *Radiat Prot Dosimetry* 52:311-315, 1994
- Chan PC, Lisco E, Lisco H, et al: The radiotoxicity of iodine-125 in mammalian cells. II. A comparative study on cell survival and cytogenetic responses to  $^{125}\text{I}$ UdR,  $^{131}\text{I}$ UdR, and  $^3\text{HTdR}$ . *Radiat Res* 67:332-343, 1976
- Bloomer WD, McLaughlin WH, Neirinckx RD, et al: Astatine-211-tellurium radiocolloid cures experimental malignant ascites. *Science* 212:340-341, 1981
- Macklis RM, Kinsey BM, Kassis AI, et al: Radioimmunotherapy with alpha-particle-emitting immunoconjugates. *Science* 240:1024-1026, 1988
- Zalutsky MR, McLendon RE, Garg PK, et al: Radioimmunotherapy of neoplastic meningitis in rats using an  $\alpha$ -particle-emitting immunoconjugate. *Cancer Res* 54:4719-4725, 1994
- McDevitt MR, Barendsward E, Ma D, et al: An  $\alpha$ -particle emitting antibody ( $^{213}\text{Bi}$ J591) for radioimmunotherapy of prostate cancer. *Cancer Res* 60:6095-6100, 2000
- Ballangrud ÅM, Yang W-H, Charlton DE, et al: Response of LNCaP spheroids after treatment with an  $\alpha$ -particle emitter ( $^{213}\text{Bi}$ )-labeled anti-prostate-specific membrane antigen antibody (J591). *Cancer Res* 61: 2008-2014, 2001
- McDevitt MR, Ma D, Lai LT, et al: Tumor therapy with targeted atomic nanogenerators. *Science* 294:1537-1540, 2001
- Burki HJ, Koch C, Wolff S: Molecular suicide studies of  $^{125}\text{I}$  and  $^3\text{H}$  disintegration in the DNA of Chinese hamster cells. *Curr Top Radiat Res Q* 12:408-425, 1977
- Esteban JM, Schlom J, Mornex F, et al: Radioimmunotherapy of athymic mice bearing human colon carcinomas with monoclonal antibody B72.3: Histological and autoradiographic study of effects on tumors and normal organs. *Eur J Cancer Clin Oncol* 23:643-655, 1987
- Otte A, Mueller-Brand J, Dellas S, et al: Yttrium-90-labelled somatostatin-analogue for cancer treatment. *Lancet* 351:417-418, 1998
- Chinn PC, Leonard JE, Rosenberg J, et al: Preclinical evaluation of  $^{90}\text{Y}$ -labeled anti-CD20 monoclonal antibody for treatment of non-Hodgkin's lymphoma. *Int J Oncol* 15:1017-1025, 1999
- Axworthy DB, Reno JM, Hylarides MD, et al: Cure of human carcinoma xenografts by a single dose of pretargeted yttrium-90 with negligible toxicity. *Proc Natl Acad Sci USA* 97:1802-1807, 2000

38. DeNardo GL, Kukis DL, DeNardo SJ, et al: Enhancement of  $^{67}\text{Cu}$ -2IT-BAT-Lym-1 therapy in mice with human Burkitt's lymphoma (Raji) using interleukin-2. *Cancer* 80:2576-2582, 1997
39. Kassis AI, Sastry KSR, Adelstein SJ: Kinetics of uptake, retention, and radiotoxicity of  $^{125}\text{I}$ UdR in mammalian cells: Implications of localized energy deposition by Auger processes. *Radiat Res* 109:78-89, 1987
40. Bloomer WD, McLaughlin WH, Weichselbaum RR, et al: Iodine-125-labelled tamoxifen is differentially cytotoxic to cells containing oestrogen receptors. *Int J Radiat Biol* 38:197-202, 1980
41. Kassis AI, Fayad F, Kinsey BM, et al: Radiotoxicity of  $^{125}\text{I}$  in mammalian cells. *Radiat Res* 111:305-318, 1987
42. Walicka MA, Ding Y, Roy AM, et al: Cytotoxicity of [ $^{125}\text{I}$ ]iodoHoechst 33342: Contribution of scavengeable effects. *Int J Radiat Biol* 75:1579-1587, 1999
43. Costantini DL, Chen C, Cai Z, et al:  $^{111}\text{In}$ -labeled trastuzumab (herceptin) modified with nuclear localization sequences (NLS): An Auger electron-emitting radiotherapeutic agent for HER2/neu-amplified breast cancer. *J Nucl Med* 48:1357-1368, 2007
44. Reske SN, Deisenhofer S, Glatting G, et al:  $^{123}\text{I}$ -ITdU-mediated nanoirradiation of DNA efficiently induces cell kill in HL60 leukemia cells and in doxorubicin-,  $\beta$ -, or  $\gamma$ -radiation-resistant cell lines. *J Nucl Med* 48:1000-1007, 2007
45. Kassis AI, Kirichian AM, Wang K, et al: Therapeutic potential of 5- $^{125}\text{I}$ iodo-2'-deoxyuridine and methotrexate in the treatment of advanced neoplastic meningitis. *Int J Radiat Biol* 80:941-946, 2004
46. Mariani G, Di Sacco S, Bonini R, et al: Biochemical modulation by 5-fluorouracil and l-folinic acid of tumor uptake of intra-arterial 5- $^{123}\text{I}$ iodo-2'-deoxyuridine in patients with liver metastases from colorectal cancer. *Acta Oncol* 35:941-945, 1996
47. Bloomer WD, Adelstein SJ: 5- $^{125}\text{I}$ -iododeoxyuridine as prototype for radionuclide therapy with Auger emitters. *Nature* 265:620-621, 1977
48. Baranowska-Kortylewicz J, Makrigrigios GM, Van den Abbeele AD, et al: 5- $^{123}\text{I}$ iodo-2'-deoxyuridine in the radiotherapy of an early ascites tumor model. *Int J Radiat Oncol Biol Phys* 21:1541-1551, 1991